

Intracluster Anionic Oligomerization of Acrylic Ester Molecules Initiated by Electron Transfer from an Alkali Metal Atom

Hironori Tsunoyama, Keijiro Ohshimo, Fuminori Misaizu,* and Koichi Ohno*

Contribution from the Department of Chemistry, Graduate School of Science, Tohoku University, Aramaki, Aoba-ku, Sendai 980-8578, Japan

Received June 16, 2000

Abstract: Stabilities and intracluster reactions have been investigated by photoionization mass spectrometry for clusters composed of an alkali metal atom (M; Na and K) and acrylic ester molecules, $\text{CH}_2=\text{CHCO}_2\text{R}$, such as methyl acrylate (MA; $\text{R} = \text{CH}_3$) and ethyl acrylate (EA; $\text{R} = \text{C}_2\text{H}_5$). The following two features are commonly observed in the photoionization mass spectra of $\text{M}(\text{CH}_2=\text{CHCO}_2\text{R})_n$: (1) The ion with $n = 3$ is clearly observed as a magic number. (2) Fragmented cluster ions with the loss of ROH, $[\text{M}(\text{CH}_2=\text{CHCO}_2\text{R})_n - \text{ROH}]$ are detected only for $n = 3$. These features are both explained by an intracluster oligomerization reaction initiated by electron transfer from the metal atoms. The magic number trimer is concluded to have the stable structure of cyclohexane derivatives as a result of oligomerization. The fragmentation reaction is explained by Dieckmann cyclization after anionic oligomerization to produce another isomer of the trimer. The intracluster electron transfer is also supported by theoretical calculation for Na(MA) based on density functional theory.

1. Introduction

In recent years, the anionic polymerization of vinyl compounds in the condensed phase has received much attention as a method to obtain various useful materials.¹ It has been established that strong bases initiate anionic polymerization of vinyl compounds that bear electron-withdrawing substituents, such as cyano (CN) and carboxyl (CO_2R) groups. An electron transfer from these strong bases causes cleavage of the $\text{C}=\text{C}$ double bond of the vinyl monomer to yield a carbanion. Thus, the contact ion pair of the vinyl molecular anion and its counterion is expected to be produced in the initial step of the polymerization, even though the pair is subsequently separated as a result of solvation in the bulk solution. The carbanion then reacts with another monomer to produce a carbanion with a longer chain as a propagating species. Various types of strong bases, such as alkali metals and alkyllithium molecules, have been used for the condensed phase, and their performances have been studied.²

However, the microscopic role of electron-donative species in anionic polymerization has not been well elucidated in terms of elementary reaction processes. For this purpose, gas-phase studies should have some advantages from the following features: (1) it is possible to discuss reactivity which is free from the solvent effect, and (2) assignment and the time evolution of the sequentially polymerized products are directly obtained by the mass spectrometric method. In recent years, anionic oligomerization in the gas phase has been studied to some extent,^{3–13} as well as cationic oligomerization.^{14–21}

As one of the gas-phase studies, a flowing ion–molecule reaction was investigated to elucidate the reaction mechanism of anionic oligomerization.^{3,4} McDonald and Chowdhury applied negative ions such as F_3C^- , NCCH_2^- , and C_3H_5^- as the reaction initiator in the gas-phase flowing afterglow apparatus.³ As for methyl acrylate (MA; $\text{CH}_2=\text{CHCO}_2\text{CH}_3$), McDonald and Chowdhury investigated the reaction mechanism by the mass spectrometric method, and they found that oligomerization terminates at the trimer, irrespective of the reaction initiator in the ion–molecule reactions. They concluded that this termination should be attributed to the following two competitive processes: (1) Dieckmann cyclization followed by loss of $\text{CH}_3\text{-OH}$ to form a conjugate base of cyclized β -keto ester and (2)

- (5) Tsukuda, T.; Kondow, T. *J. Am. Chem. Soc.* **1994**, *116*, 9555.
- (6) Tsukuda, T.; Kondow, T. *Chem. Phys. Lett.* **1992**, *197*, 438.
- (7) Tsukuda, T.; Kondow, T. *J. Phys. Chem.* **1992**, *96*, 5671.
- (8) Tsukuda, T.; Terasaki, A.; Kondow, T.; Scarton, M. G.; Dessent, C. E.; Bishea, G. A.; Johnson, M. A. *Chem. Phys. Lett.* **1993**, *201*, 351.
- (9) Fukuda, Y.; Tsukuda, T.; Terasaki, A.; Kondow, T. *Chem. Phys. Lett.* **1996**, *260*, 423.
- (10) Ichihashi, M.; Tsukuda, T.; Nonose, S.; Kondow, T. *J. Phys. Chem.* **1995**, *99*, 17354.
- (11) Fukuda, Y.; Tsukuda, T.; Terasaki, A.; Kondow, T. *Chem. Phys. Lett.* **1995**, *242*, 121.
- (12) Tsukuda, T.; Kondow, T.; Dessent, C. E. H.; Bailey, C. G.; Johnson, M. A.; Hendricks, J. H.; Lyapustina, S. A.; Bowen, K. H. *Chem. Phys. Lett.* **1997**, *269*, 17.
- (13) Ohshimo, K.; Misaizu, F.; Ohno, K. *J. Phys. Chem. A* **2000**, *104*, 765.
- (14) El-Shall, M. S.; Yu, Z. *J. Am. Chem. Soc.* **1996**, *118*, 13058.
- (15) Coolbaugh, M. T.; Whitney, S. G.; Vaidyanathan, G.; Garbey, J. F. *J. Phys. Chem.* **1992**, *96*, 9139.
- (16) El-Shall, M. S.; Daly, G. M.; Yu, Z.; Meot-Ner (Mautner), M. J. *Am. Chem. Soc.* **1995**, *117*, 7744.
- (17) El-Shall, M. S.; Marks, C. J. *J. Phys. Chem.* **1991**, *95*, 4932.
- (18) Daly, G. M.; Pithawalla, Y. B.; Yu, Z.; El-Shall, M. S. *Chem. Phys. Lett.* **1995**, *237*, 97.
- (19) Brodbelt, J. S.; Liou, C. C.; Maleknia, S.; Lin, T. Y.; Lagow, R. J. *J. Am. Chem. Soc.* **1993**, *115*, 11069.
- (20) Wang, J.; Javahery, G.; Petrie, S.; Bohme, D. K. *J. Am. Chem. Soc.* **1992**, *114*, 9665.
- (21) Pithawalla, Y. B.; Gao, J.; Yu, Z.; El-Shall, M. S. *Macromolecules* **1996**, *29*, 8558.

* Corresponding authors: (e-mail) misaizu@qpcrkk.chem.tohoku.ac.jp; ohnok@qpcrkk.chem.tohoku.ac.jp.

(1) Hogen-Esh, T. E.; Smid, J. *Recent Advances in Anionic Polymerization*; Elsevier: New York, 1987.

(2) Tsuruta, T., O'Driscoll, K. F., Eds. *Structure and Mechanism in Vinyl Polymerization*; Marcel Dekker: New York, 1969.

(3) McDonald, R. N.; Chowdhury, A. K. *J. Am. Chem. Soc.* **1983**, *105*, 2194.

(4) McDonald, R. N.; Chowdhury, A. K. *J. Am. Chem. Soc.* **1982**, *104*, 2675.

intramolecular H⁺ transfer to produce the isomeric unreactive anion. The relative amounts of these two termination reactions were found to be strongly dependent on the structure of the initiator anion. Several side reactions were also observed when NCC₂⁻ and C₃H₅⁻ were used as initiators.

Studies on gas-phase clusters were also performed as models of the anionic oligomerization reaction.^{5–13} These studies can be classified by the types of the electron-donative species used as initiators for the oligomerization reactions. One of the simplest microscopic models for the initial step of anionic oligomerization is the system of a free anion of the vinyl molecule and other monomers, that is, a cluster anion of vinyl compound. Tsukuda and Kondow and their co-workers have extensively investigated cluster anions of vinyl compounds produced by electron transfer from high-Rydberg rare gas atoms.^{5–7} Photodissociation spectroscopy,^{8,9} collision-induced dissociation,¹⁰ and photoelectron spectroscopy^{11,12} of the cluster anions were also employed in their studies. Trimeric terminations were also observed for cluster anions of acrylonitrile (AN; CH₂=CHCN) and its derivatives.⁵ They concluded that the trimeric unit is a stable anion radical that has a cyclohexane ring structure. As for AN, the trimeric ring was observed to be important for the production of (AN)₆⁻ and (AN)₉⁻ as well as (AN)₃⁻.^{9–11} In addition to the trimeric units with cyclohexane rings, Tsukuda and Kondow observed some side reactions into a cyclohexene ring, a cyclohexadiene ring, and a benzene ring, with respective losses of fragment molecules.⁵ On the other hand, as for MA cluster anions, (MA)_n⁻, no pronounced signal (magic number) was observed at *n* = 3. In fact the pentamer, (MA)₅⁻, was found to have the most enhanced signal in the mass spectrum.⁶

The contact ion pair consisting of a vinyl anion and a counterion is also expected to be another model for the initial step of anionic oligomerization. Clusters of an initiator species and vinyl compounds can be studied as such contact ion pairs in order to discuss the mechanism of the propagation reaction of the ion pair with another monomer. In the authors' group, intracuster reactions have been investigated for clusters containing vinyl compounds and an alkali atom by means of a time-of-flight (TOF) mass spectrometer with a cluster beam source.¹³ In contrast with the studies by McDonald and Chowdhury and Tsukuda and Kondow, evidence of anionic oligomerization has been found for the neutral clusters in which the electron transfer to vinyl molecules from an alkali atom plays the key role in the reaction. In the case of neutral clusters containing alkali metal atoms (M = Li, Na and K) and AN molecules, M(AN)_n, the magic numbers at *n* = 3*k* (*k* = 1–3) was observed in their photoionization mass spectra.¹³ It should be noted that the trimeric unit with a cyclohexane ring is produced by anionic oligomerization initiated by the electron transfer from an alkali atom. These cluster systems were found to be suitable to investigate the site-specific and electronic effects of the counterion (base cation) on the initial reaction processes of the bulk polymerization reactions.

In this study, we have investigated clusters containing the alkali metal atom (Na, K) and acrylic ester molecules [CH₂=CHCO₂R (R = CH₃, C₂H₅)] by photoionization mass spectrometry. The intracuster oligomerization reaction caused by electron transfer from the alkali atom to the molecules was discussed from the size distributions observed in the mass spectra. We have discussed the intracuster reaction process by comparing the present results with previous studies of cluster anions by Tsukuda and Kondow⁶ and ion–molecule reactions by McDonald and Chowdhury.³ We have also performed the

quantum chemical calculation based on density functional theory (DFT) to obtain further insight into the intracuster reaction initiated by the alkali metal atom.

2. Experimental Section

The present experiments were performed by using apparatus described elsewhere.¹³ Briefly, the system is composed of two-stage differentially evacuated chambers which contain a cluster beam source and a Wiley–McLaren type time-of-flight mass spectrometer (TOF-MS).²² The pressures of the source and the TOF-MS chambers were maintained at about 2 × 10⁻⁵ and 7 × 10⁻⁷ Torr, respectively, during measurements. Clusters of an alkali atom and acrylic ester molecules, M(CH₂=CHCO₂R)_n (M = Na, K; R = CH₃, C₂H₅), were produced by a pickup source^{23–25} consisting of a combination of laser vaporization²⁶ and pulsed supersonic expansion. A sample gas mixed with helium (Nihon Sanso, 99.9999% pure) was expanded from a pulsed valve (General Valve, series 9, orifice diameter 0.8 mm) with a stagnation pressure of 4 atm. The second harmonic output of a Nd:YAG laser (Lumonics, HY-400, 532 nm) was focused onto a sample metal rod, which was rotated and translated for stabilizing the vaporizing conditions and placed at ~10 mm downstream from the nozzle. In this study, the vaporized metal atoms immediately collide and react with the molecular clusters formed in the pulsed jet. The resultant neutral species were introduced to the TOF-MS chamber after collimation with a conical skimmer (throat diameter of 1 mm) positioned ~30 mm downstream from the nozzle.

The neutral clusters were ionized by irradiation with a pulsed laser beam in the source region of the TOF-MS setup at 230 mm downstream from the nozzle. As a photoionization light source, we used a frequency-doubled output of a dye laser (Lumonics, HD-300 and HT-1000) pumped by a Nd:YAG laser (Spectra-Physics, GCR-150-10). To avoid multiphoton ionization processes the fluence of the ionization laser was kept under 4 mJ cm⁻² during the measurement. We measured the ionizing laser power dependence of photoion intensity and confirmed that this ionization is a one-photon process. The timing of the valve opening and both the vaporization and ionization laser irradiation was optimized using a digital delay/pulse generator (Stanford Research, DG535). The cluster ions formed by photoionization were accelerated by static electric fields to ~3.0 keV at right angles to the direction of both the cluster beam and the ionization laser. The width of Stark shift caused by field ionization, which could not be avoided under the continuous acceleration field, was estimated to be ~0.02 eV in this condition. The accelerated ions were introduced to a field-free tube of 550-mm length. The mass-separated ions were detected by a dual-microchannel plate (Hamamatsu, F1552–21S), and the output signals were stored and averaged by a digital storage oscilloscope (LeCroy, 9344C). The data stored in the oscilloscope were sent to a personal computer (NEC, PC-9801DA) via a GPIB computer interface.

Mass spectra of the cluster ions nascently formed in the cluster source were also measured concurrently with the above measurement. Cluster ions were generated by ion–molecule reactions between alkali metal ions formed by laser vaporization and neutral acrylic ester clusters in the expansion region of the free jet. The product cations were introduced to the acceleration region of the TOF-MS and accelerated to ~1.3 keV by pulsed electric fields generated by a high-voltage pulse generator (DEI, GRX-1.5K-E). The timing of the acceleration field pulse with respect to the others was also optimized with the digital delay/pulse generator.

The sample rods of sodium (Rare metallic, 99.9% pure) and potassium (Aldrich, 99.5% pure) were made under a nitrogen atmosphere in a vacuum drybox to avoid reaction with water in the air. Chemicals were purchased at the following minimum percent impurities

(22) Wiley, W. C.; McLaren, I. H. *Rev. Sci. Instrum.* **1955**, *26*, 1150.

(23) Schulz, C. P.; Haugstatter, R.; Tittes, H. U.; Hertel, I. V. *Phys. Rev. Lett.* **1986**, *57*, 1703.

(24) Schulz, C. P.; Haugstatter, R.; Tittes, H. U.; Hertel, I. V. *Z. Phys. D* **1988**, *10*, 279.

(25) Misaizu, F.; Sanekata, M.; Tsukamoto, K.; Fuke, K. *J. Phys. Chem.* **1992**, *96*, 8259.

(26) Dietz, T. G.; Duncan, M. A.; Powers, D. E.; Smalley, R. E. *J. Chem. Phys.* **1981**, *74*, 6511.

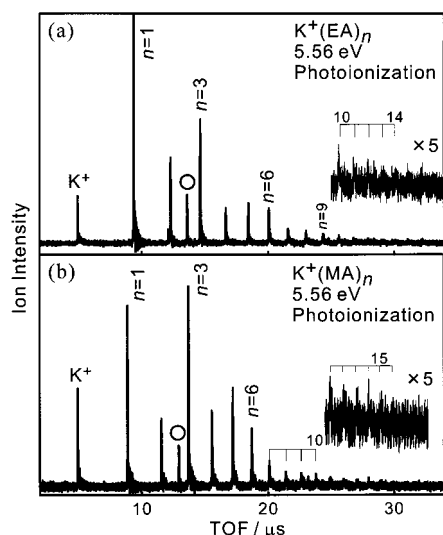


Figure 1. Typical photoionization mass spectra of (a) $K^+(EA)_n$ and (b) $K^+(MA)_n$. The ionization energy was 5.56 eV. The series of cluster ions $K^+(EA)_n$ and $K^+(MA)_n$ are predominantly observed up to $n = 14$ and 16, respectively. In both mass spectra, the peaks of $[M(\text{CH}_2=\text{CHCO}_2\text{R})_3 - \text{ROH}]^+$ ($\text{R} = \text{C}_2\text{H}_5, \text{CH}_3$; O) were also assignable.

and used without further purification: MA (Aldrich, 99% pure), ethyl acrylate (EA; Wako, 97% pure), ethyl propionate (EP; Wako, 97% pure), and methyl propionate (MP; Wako, 98% pure). The mixing ratio of MA and EA in He gas was estimated to be 3.3 and 1.3%, respectively.

3. Calculation

The quantum chemical calculations for free MA and $\text{Na}(\text{MA})$ were performed to examine the possibility of intracuster electron transfer. All calculations were carried out by using a DFT program of the Gaussian 94 package.²⁷ The 6-31+G* basis set and the B3LYP functional²⁸ were utilized in these calculations. For a free MA molecule, two conformational isomers, s-cis and s-trans, are estimated to be in an equilibrium with a relative abundance of s-cis:s-trans = 67:33 at room temperature.²⁹ Therefore, we performed a geometrical optimization calculation of MA and $\text{Na}(\text{MA})$ only for the s-cis conformer. The calculated bond lengths and angles of s-cis MA showed excellent agreement (within 0.007 Å and 0.8°) with those determined by electron diffraction data and rotational constants.²⁹ In the structural optimization for $\text{Na}(\text{MA})$, some of the geometrical parameters in MA were fixed to those of the optimized free MA molecule as shown in section 4F. The electron density of the $\text{Na}(\text{MA})$ was also calculated to discuss the intracuster electron transfer.

4. Results and Discussion

A. Size Distribution in Photoionization Mass Spectra of $K^+(EA)_n$ and $K^+(MA)_n$. Typical mass spectra obtained by photoionization of $K^+(EA)_n$ and $K^+(MA)_n$ by irradiation with a laser beam of 5.56 eV are shown in Figure 1. In this figure, the series

(27) Frisch, M. J.; Trucks, G. W.; Schlegel, H. B.; Gill, P. M. W.; Johnson, B. G.; Robb, M. A.; Cheeseman, J. R.; Keith, T.; Petersson, G. A.; Montgomery, J. A.; Raghavachari, K.; Al-Laham, M. A.; Zakrzewski, V. G.; Ortiz, J. V.; Foresman, J. B.; Cioslowski, J.; Stefanov, B. B.; Nanayakkara, A.; Challacombe, M.; Peng, C. Y.; Ayalla, P. Y.; Chen, W.; Wong, M. W.; Andres, J. L.; Replogle, E. S.; Gomperts, R.; Martin, R. L.; Fox, D. J.; Binkley, J. S.; Defrees, D. J.; Baker, J.; Stewart, J. P.; Head-Gordon, M.; Gonzalez, C.; Pople, J. A. *Gaussian 94*, Revision E.2; Gaussian, Inc.: Pittsburgh, PA, 1995.

(28) Becke, A. D. *J. Chem. Phys.* **1993**, *98*, 5648.

(29) Egawa, T.; Maekawa, S.; Fujiwara, H.; Takeuchi, H.; Konaka, S. *J. Mol. Struct.* **1995**, *352/353*, 193.

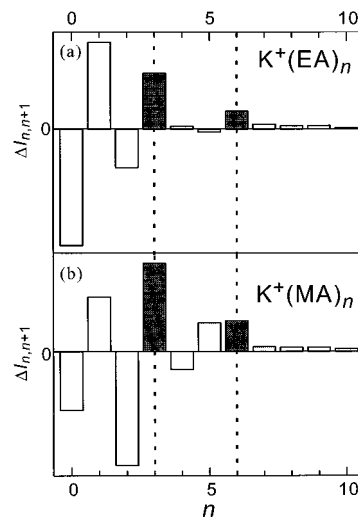


Figure 2. Ion intensity difference between $K^+(\text{CH}_2=\text{CHCO}_2\text{R})_n$, $I(n)$, and $K^+(\text{CH}_2=\text{CHCO}_2\text{R})_{n+1}$, $I(n+1)$, $\Delta I_{n,n+1} = I(n) - I(n+1)$ plotted against cluster size n . (a) $K^+(\text{EA})_n$ ($\text{R} = \text{C}_2\text{H}_5$) and (b) $K^+(\text{MA})_n$ ($\text{R} = \text{CH}_3$).

of cluster ions of $K^+(EA)_n$ and $K^+(MA)_n$ are mainly observed up to $n = 14$ and 16, respectively. These clusters were ionized by absorption of a single 5.56-eV photon, because ionization energy of the K atom is only 4.34 eV,³⁰ and in general these clusters have lower ionization threshold energies than K atoms. Two significant features common to these two systems are observed as follows. First, the same intensity anomalies (magic numbers) at $n = 3$ and 6 are found in the size distribution of $K^+(EA)_n$ and $K^+(MA)_n$ series. The intensities of $K^+(EA)_3$ and $K^+(MA)_3$ are both more than 2 times higher than those of $K^+(EA)_2$ and $K^+(MA)_2$, respectively. Another intensity anomaly at $n = 6$ is easily observed in the plots of the difference between the areal intensity of $K^+(\text{EA or MA})_n$, $I(n)$, and that of $K^+(\text{EA or MA})_{n+1}$, $I(n+1)$, $\Delta I_{n,n+1} = I(n) - I(n+1)$, as shown in Figure 2. In this figure, $\Delta I_{n,n+1}$ are found to be larger for $n = 6$ than for adjacent sizes, in addition to $n = 3$ for both systems. Another common feature is that the peaks caused by the loss of $\text{C}_2\text{H}_5\text{OH}$ or CH_3OH are observed only from the trimer ions $K^+(\text{EA})_3$ and $K^+(\text{MA})_3$; the fragment ions are observed only at $m/z = 293$ [$K^+(\text{EA})_3 - \text{C}_2\text{H}_5\text{OH}$] for the K-EA system and at $m/z = 265$ [$K^+(\text{MA})_3 - \text{CH}_3\text{OH}$] for the K-MA system. These two features are independent of the wavelength of the ionizing laser in the region between 4.66 and 5.56 eV.

B. Size Distribution in Photoionization Mass Spectra of $\text{Na}(\text{EA})_n$ and $\text{Na}(\text{MA})_n$. We also measured the photoionization mass spectra of clusters containing Na atom and acrylic ester as shown in Figure 3. The photon energy was 5.56 eV for one-photon ionization of $\text{Na}(\text{MA})_n$ and $\text{Na}(\text{EA})_n$. In Figure 3a, the series of cluster ions of $\text{Na}^+(\text{EA})_n$ is predominantly observed up to $n = 7$. The peak caused by loss of $\text{C}_2\text{H}_5\text{OH}$ from the $n = 3$ cluster ion is also observed as it is for $K^+(\text{EA})_n$ (Figure 1a). In Figure 3b, the series of cluster ions of $\text{Na}^+(\text{MA})_n$ is mainly observed up to $n = 6$ and the peak caused by loss of CH_3OH from the $n = 3$ cluster ion is again observed. In these mass spectra, the magic number behavior at $n = 3$ is again observed as with $K^+(\text{MA})_n$ (Figure 1b). The two features mentioned above for potassium complexes are therefore also observed for sodium systems, and the presence of the magic number at $n = 3$ and loss of ROH from $n = 3$ cluster appear to be common features for the alkali metal-acrylic ester clusters, $M(\text{CH}_2=\text{CHCO}_2\text{R})_n$.

(30) Moore, C. E. *Atomic Energy Levels*; United States Department of Commerce, National Bureau of Standards: Washington, DC, 1949; Vol. I.

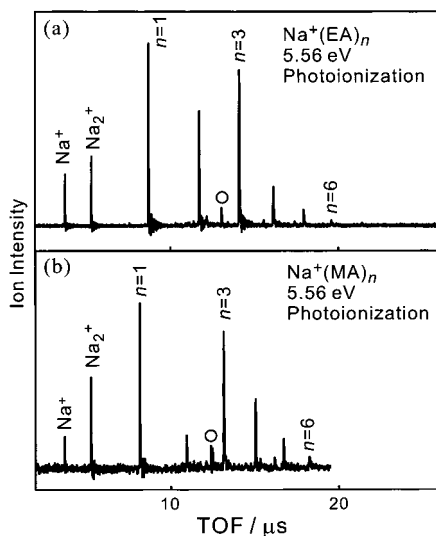


Figure 3. Typical photoionization mass spectra of (a) $\text{Na}^+(\text{EA})_n$ and (b) $\text{Na}^+(\text{MA})_n$. The ionization energy was 5.56 eV. The series of cluster ions $\text{Na}^+(\text{EA})_n$ and $\text{Na}^+(\text{MA})_n$ are predominantly observed up to $n = 7$ and 6, respectively. In both mass spectra, the peaks of $[\text{M}(\text{CH}_2=\text{CHCO}_2\text{R})_3 - \text{ROH}]^+$ ($\text{R} = \text{C}_2\text{H}_5, \text{CH}_3; \text{O}$) were also assignable.

The ions of sodium clusters solvated with EA or MA, such as $\text{Na}_m^+(\text{EA})_n$ ($m \geq 2$), are not observed in these mass spectra, whereas Na_2^+ ion signal is detected. This tendency is a feature of the pickup source because there is no channel for the growth of metal clusters in front of the pulsed valve. For example, in the photoionization mass spectroscopy of $\text{Na}_m(\text{H}_2\text{O})_n$ using the pickup source, the series of $m = 2$ is reported to be very weakly observed along with that of $m = 1$.²⁴

C. Appearance of Magic Numbers. In our cluster source, the metal atom–molecule clusters are expected to be produced by collision of the vaporized metal atoms with molecular clusters preformed by supersonic expansion, although subsequent collisional processes with buffer He gas or metal vapor cannot be ruled out. We have also examined mass spectrometry of the cluster ions nascently produced in the source. In the latter case, the cluster ions are produced by collision between the preformed molecular clusters and the metal atom ions. Examples of these results are shown in Figure 4 for $\text{K}^+(\text{EA})_n$ and $\text{K}^+(\text{MA})_n$. In these mass spectra, it is expected that the observed size distributions depend on the stability of ions produced by such ion–molecule (cluster) reactions. The series of $\text{K}^+(\text{EA})_n$ and $\text{K}^+(\text{MA})_n$ cluster ions are observed up to $n = 6$ and 9, respectively. The ion intensities are found to decrease monotonically with increasing n in these mass spectra, without magic-number behavior at $n = 3$ and 6. These results indicate that the cluster ions at $n = 3$ and 6 are not more stable than adjacent sizes. Therefore, the magic numbers observed in the photoionization of neutral clusters possibly originate from the following two processes:¹³ (1) collisional complex formation between the neutral alkali atom with acrylic ester clusters and (2) photoionization of the neutral metal atom–acrylic ester clusters. In process 1, magic numbers are formed by the relative stability of neutral alkali atom–acrylic ester clusters. On the other hand, two factors are considered in generating magic numbers for process 2: (2-1) the photoionization efficiency of neutral clusters that is dependent on the photon energy for ionization and (2-2) the evaporation processes after ionization that depend on the stability of cluster ions. For (2-2), ions formed by photoionization may have enough energy to dissociate intermolecular bonds in the cluster ions. If the evaporation processes take place efficiently after photoionization, relatively stable ions will tend

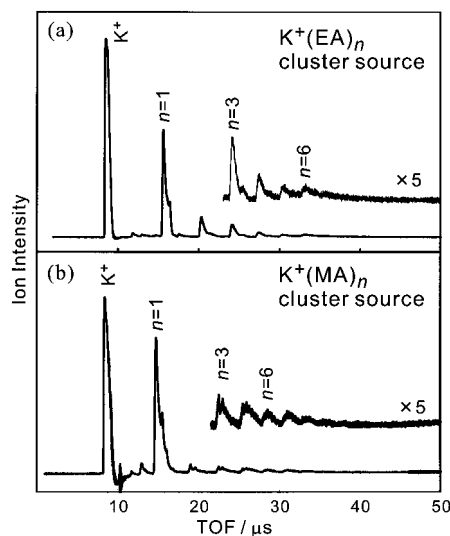


Figure 4. Typical mass spectra of (a) $\text{K}^+(\text{EA})_n$ and (b) $\text{K}^+(\text{MA})_n$ produced by ion–molecule reaction in the cluster source. The series of cluster ions of $\text{K}^+(\text{EA})_n$ and $\text{K}^+(\text{MA})_n$ are predominantly observed up to $n = 6$ and 9, respectively.

Table 1. Ionization Threshold Energies (IE) of $\text{K}(\text{EA})_n$

n	IE (eV)	n	IE (eV)
0	4.34 ^a	3	3.60(12)
1	4.35(7)	4	3.81(9)
2	3.90(4)		

^a Reference 30.

to be populated by evaporation from less stable ions, and as a result, the n -dependent stability of ions is expected to be reflected by the size distribution in the photoionization mass spectrum. Although size distribution of the cluster ions formed in the source shows no evidence for the size-dependent stability corresponding to the observed magic numbers, the ions produced by photoionization may have different structures, that is, size-dependent stabilities different from those formed by ion–molecule reaction. Next we will discuss these possibilities.

To discuss the possibilities of (2-1) and (2-2), it is important to know the ionization thresholds of metal atom–acrylic ester clusters. By scanning the ionization laser wavelength, we have measured the thresholds for ionization of $\text{K}(\text{EA})_n$ clusters of $n = 1-4$. From the results shown in Table 1, the clusters for $n \geq 2$ are found to have ionization threshold energies in the region of 3.6–3.9 eV. Because the magic number behavior at $n = 3$ and 6 is observed at a photon energy that is high enough with respect to the ionization thresholds of these clusters, we feel safe in ruling out the possibility 2-1 by assuming that the ionization efficiency is almost constant or at least not sensitively dependent on n for all clusters in the present mass spectra. On the other hand, the possibility of evaporation processes 2-2 is also not expected to be serious, because the magic numbers are also observed at the photon energy of 4.66 eV, which is only about 0.7–1.0 eV above the ionization thresholds. Calculated dissociation energy for $\text{Na}^+(\text{MA})$ is estimated to be more than 1.4 eV,³¹ so that the evaporation process is insignificant at this photon energy. After all, we concluded that hypothesis 1 is most probable; the magic numbers can be related to the nature of neutral alkali atom–acrylic ester clusters.

D. Structures of the Magic Number Clusters, $\text{M}(\text{CH}_2=\text{CHCO}_2\text{R})_3$. Now we consider possible structures of neutral

(31) Tsunoyama, H.; Ohshimo, K.; Misaizu, F.; Ohno, K. Unpublished results.

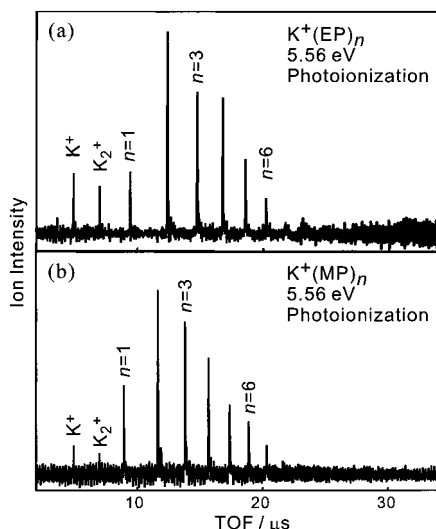


Figure 5. Typical photoionization mass spectra of (a) $K(EP)_n$ and (b) $K(MP)_n$. The ionization energy was 5.56 eV. The series of cluster ions of $K^+(EP)_n$ and $K^+(MP)_n$ are predominantly observed up to $n = 8$ in both mass spectra.

$M(CH_2=CHCO_2R)_3$ clusters. Clusters consisting of a metal atom and molecules have been studied in connection with solvation in electrolyte solution for the past decade.^{23,24,32–35} Among these studies, clusters of alkali atoms solvated with polar molecules such as water or ammonia is one of the main targets, mainly because intracuster electron transfer from the metal atom to molecules is expected in this system as a model of the bulk solution forming solvated electrons.^{32,33} All such clusters have a structures for which one metal atom or ion is solvated by solvent molecules. By contrast, the present observation of magic number behavior cannot be explained by considering the solvation structure (solvation shell) in the neutral clusters. This is because, in the solvation-type structures, the stability of the cluster is expected to be sensitively dependent on the atomic radii of solvated alkali atoms, which are, for example, 1.86 and 2.27 Å for Na and K, respectively.³⁶ The fact that the magic number behavior at $n = 3$ is commonly observed for Na and K clusters indicates that the stability of the present clusters is not determined by the solvation structure. It is rather expected that they can be attributed to the formation of a chemical bond (intracuster reaction) due to the electron configuration of the metal atom. In other words, the ns valence electron of the alkali metal atom plays a crucial role in the formation of magic number clusters. These features are also common to the acrylic ester species, EA and MA, as constituent molecules. In comparison, we have also obtained the photoionization mass spectra of clusters of a K atom with EP ($CH_3CH_2CO_2C_2H_5$) and MP ($CH_3CH_2CO_2CH_3$), which have structures similar to EA and MA, respectively, but without C=C bonds (Figure 5). In these mass spectra, the size distributions of $K^+(EP)_n$ and $K^+(MP)_n$ are found to be rather smooth with no features observed in M–EA and M–MA clusters. Therefore, the existence of the C=C bond is also shown to have a critical role in the emergence of magic numbers.

(32) Schulz, C. P.; Hertel, I. V. In *Clusters of Atoms and Molecules II*; Haberland, H., Ed.; Springer-Verlag: Berlin-Heidelberg, 1994.

(33) Fuke, K.; Hashimoto, K.; Iwata, S. *Adv. Chem. Phys.* **1999**, *110*, 431.

(34) Ohshimo, K.; Tsunoyama, H.; Yamakita, Y.; Misaizu, F.; Ohno, K. *Chem. Phys. Lett.* **1999**, *301*, 356.

(35) Tsunoyama, H.; Ohshimo, K.; Yamakita, Y.; Misaizu, F.; Ohno, K. *Chem. Phys. Lett.* **2000**, *316*, 442.

(36) Emsley, J. *The Elements*, 3rd ed.; Oxford University Press: New York, 1998.

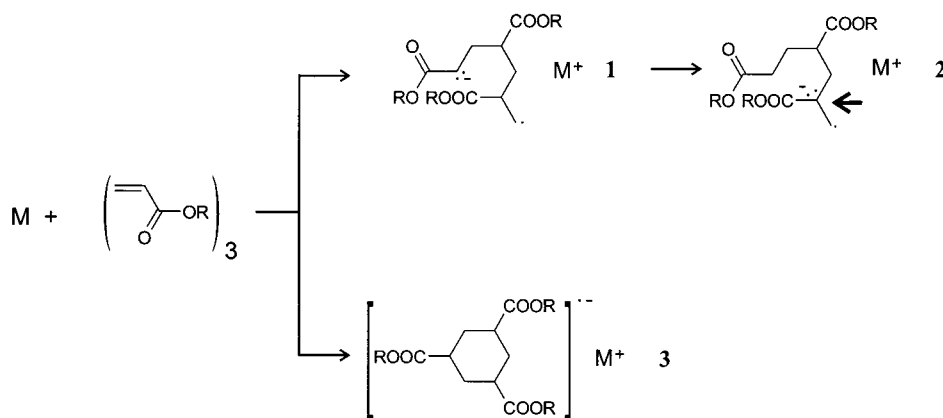
Next we discuss possible intracuster reactions and resultant structures of $M(CH_2=CHCO_2R)_n$. From the results noted above, it is expected that electron transfer from the alkali atom to acrylic ester molecules should induce an intracuster oligomerization reaction. This hypothesis comes from the anionic polymerization reaction seen in the bulk solution and is also supported by the results of theoretical calculation for the Na(MA) cluster as shown in section 4F. It is further reported that charge transfer from an initiator to vinyl monomer initiates the cationic oligomerization.¹⁴ The reaction process of anionic polymerization initiated by alkali metals has the following two steps: (1) electron transfer from the metal atom to the monomer; (2) the ion pair formed by step 1 reacts with another monomer. In this step, 1,4-addition is considered to be possible as discussed in the ion–molecule reaction study by McDonald and Chowdhury.³ In the intracuster oligomerization reaction initiated by electron transfer from the metal atom, we consider the three different products for $M(CH_2=CHCO_2R)_3$ shown in Scheme 1.

The species **1** and **2** are formed by successive reactions observed in the study by McDonald and Chowdhury.³ The structure **1** is formed by a three-step reaction: electron transfer from the alkali atom to a monomer and two successive conjugate 1,4-additions. These successive additions (propagation steps) are terminated by producing a stable anion which is unreactive with additional monomer. In the ion–molecule reaction study by McDonald and Chowdhury,³ this structure is not especially stable at $n = 3$ because **1** undergoes two competitive intramolecular reactions forming unreactive species: intramolecular H^+ transfer giving the isomeric enolate anion **2** and Dieckmann cyclization with the loss of a ROH molecule. Therefore, structure **1** is not considered to be particularly stable at $n = 3$ and cannot explain the magic number behavior. However, this structure is still important in the formation processes of fragment ions observed in the mass spectra as discussed in the next section. In the study by McDonald and Chowdhury,³ **2** is stabilized by the substituent effect of electron-withdrawing groups (CH_2CF_3) at the α -carbon indicated by an arrow in the Scheme 1. There is no substituent effect to stabilize the trimer in the present case, so this structure cannot explain the magic number either.

Finally, we consider structure **3** in Scheme 1. The same magic number behavior at $n = 3k$ ($k = 1–3$) was also observed in $M(AN)_n$ and $(AN)_n^-$ clusters. The cyclic trimerization reaction (intracuster oligomerization) occurs in both cases.^{5,13} This reaction was initiated by electron transfer from a metal atom in the former and from a high-Rydberg rare gas atom in the latter. In the present system, this reaction can also occur and produces an anion radical of a stable molecule which is assignable to trimethyl- (or triethyl-) 1,3,5-cyclohexanetricarboxylate. This structure of the neutral cluster at $n = 3$ is more stable than other sizes because of the lack of ring strain as discussed in the preceding papers.^{5,13} The same magic number behavior was also reported for acetylene¹⁵ and isobutene¹⁶ cluster cations in the study of gas-phase cationic oligomerization. As a result of the evaporation process from the clusters for $n \geq 3$ after the reaction, the population of the $M(CH_2=CHCO_2R)_3$ cluster increases because monomers cannot be further evaporated from this stable species. To confirm the intracuster cyclization process, we have examined the stability of $M(AN)_n$ by photodissociation of the neutral clusters before ionization.³⁷ Visible laser was irradiated with the neutral clusters and induced the evaporation process of unreacted AN within the clusters. In the preliminary experiments, the population of the $n = 3$ cluster was found to

(37) Ohshimo, K.; Tsunoyama, H.; Misaizu, F.; Ohno, K. Unpublished results.

Scheme 1



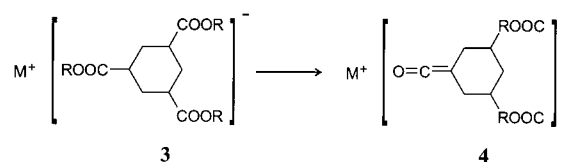
increase in the mass spectrum when the visible laser was on. This result also suggests that stable trimer units such as structure **3** are produced for $n \geq 3$ clusters.

In addition, for the photoionization mass spectra of $K(EA)_n$ and $K(MA)_n$, a magic number at $n = 6$ is also observed (Figure 1). This feature resembles that observed in $M-AN$ clusters.¹³ It is suggested that two cyclic trimer units are formed at $n = 6$. Therefore, it is confirmed again that the magic number behavior at $n = 3$ is attributed to the cyclization reaction to form **3** and that at $n = 6$ is assigned to the cyclization reaction forming two cyclic units. Although the electronic states of the reaction products for cyclic trimer **3** are unclear, it is suggested that the unpaired electrons in the products have possibilities to return to M^+ . In the condensed phase, the return of an electron to M^+ (neutralization of cation) is suggested to be one of the termination reactions of anionic polymerization.³⁸ Therefore, from the observed magic number at $n = 6$, it is suggested that the returned electron transfers again from the metal atom to unreacted acrylic ester molecules and initiates another oligomerization reaction.

E. Fragmentation Process from the Trimer. To discuss the dissociation mechanism of ROH from $n = 3$ clusters, we first consider the possibility of fragmentation on the ionic potential surface with the excess energy after photoionization. The appearance threshold energy of the fragmentation product ion, $[K(EA)_3 - C_2H_5OH]^+$, was determined to be 4.37 eV for the $K-EA$ system. Because the ionization threshold energy of $K(EA)_3$ is 3.60 eV as shown in Table 1, the minimum energy necessary for the dissociation reaction is as low as 0.8 eV, assuming that the fragment ion is produced from $K^+(EA)_3$. However, it is known that the C-OR bond dissociation energy amounts to ~ 4 eV.³⁹ Thus, in the present case, the process of dissociation after ionization is ruled out. It is probable that the fragmentation reaction proceeds from the neutral $M(CH_2=CHCO_2R)_3$ and is induced by the electron transfer from the metal atom, as in the oligomerization reaction producing the cyclic trimer.

Next we consider the relationship between two reactions, the fragmentation and the oligomerization, to produce the stable trimer. In other words, the problem is whether fragmentation may proceed from the cyclic trimer or not. The cyclization reaction at $n = 3$ is exothermic so that the heat of reaction may cause the dissociation of the chemical bond. For example, the dissociation of HCl from the $n = 3$ cluster was observed in the mass spectrometric study of chloroacrylonitrile anion clusters.^{5,7,8,12} This dissociation reaction, caused by the heat of the

Scheme 2



cyclization reaction, produces a stable 1,3,5-tricyanobenzene molecule. Also in the AN anion clusters, the dissociation of the hydrogen atoms or HCN from cyclic trimer is found to be caused by the excess energy generated by the exothermic oligomerization.⁵ This explanation holds for the electron attachment process under collision-free conditions. By contrast, in our cluster source, the excess energy given by the intracuster oligomerization of vinyl molecules can be removed by multiple collision between the He buffer gas and the clusters, as noted in section 4C. In a study of $M(AN)_n$ ($M = Li, Na, K$), in which the same cluster source was used as in the present study, the elimination of hydrogen atoms or HCN was hardly observed in the photoionization mass spectra.¹³ In the present case, dissociation of ROH from the cyclic trimer **3** may produce a ketene derivative (Scheme 2).

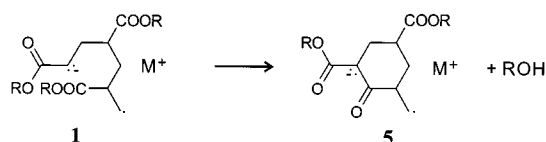
This reaction is expected to be endothermic, because ketene derivatives are in general unstable and highly reactive. Endothermic reactions are presumed to be suppressed in the present source condition as noted above. Moreover, if sufficient energy remains in the cyclic trimer **3** to produce a ketene derivative, it is expected that various fragmentation reactions other than ROH elimination would be observed. Therefore, dissociation from the cyclic trimer caused by excess energy can be ruled out and another dissociation reaction mechanism should be considered that is competitive with the formation of **3** at $n = 3$ after electron transfer.

In the ion-molecule reaction study by McDonald and Chowdhury,³ the product ion formed by loss of ROH from the trimer was also observed. This dissociation reaction was explained by Dieckmann cyclization, which is known as a condensation reaction of diester to produce an enolate anion of cyclized β -keto ester. In the present case, structure **1** in Scheme 1 is expected to be a reactant of the Dieckmann cyclization. The product of this reaction (**5** in Scheme 3) is a six-membered cyclized β -keto ester without any ring strain. It is difficult for Dieckmann cyclization to occur at other cluster sizes because of the ring strain of the products. Although the distonic radical such as product **5** may be unstable with respect to subsequent reactions, **5** is expected to be stabilized by Na^+ coordination with the carbon atom having an unpaired electron, on the basis of the calculated structure for the 1:1 complex shown in the

(38) Szwarc, M. *Nature* **1956**, *178*, 1168.

(39) Sanderson, R. T. *Chemical Bonds and Bond Energy*, 2nd ed.; Academic Press: New York, 1976.

Scheme 3



next section. Therefore, it is concluded that the dissociation reaction at $n = 3$ proceeds as follows.

Formation of the oligomer **1** followed by Dieckmann cyclization is a competitive reaction with the formation of the cyclic trimer with cyclohexane ring discussed in section 4D. In the photoionization mass spectra of $M-\text{CH}_2=\text{CHCO}_2\text{R}$ clusters (Figures 1 and 3), it is observed that the intensities of $M^+(\text{CH}_2=\text{CHCO}_2\text{R})_3$ are more than 2 times higher than those of the $[M(\text{CH}_2=\text{CHCO}_2\text{R})_3 - \text{ROH}]^+$ fragment ions for all systems examined. Therefore, the cyclohexane ring formation is expected to be dominant on the assumption that the Dieckmann cyclization process is much faster than the time window in the present experiment ($\sim 200 \mu\text{s}$). To discuss the present result further, it is necessary to know energetic information about these processes, which is not available at present.

F. Calculated Structure of Na(MA) and the Possibility of Intracuster Electron Transfer. To get further insight into the intracuster electron transfer, we have optimized the structure of Na(MA) based on DFT (B3LYP/6-31+G*). The structures obtained for the free MA molecule and for two isomers of Na(MA) (designated as **a** and **b**) are shown in Figure 6a and b, respectively. In the structural optimization for Na(MA), the rotation of C^1H_3 , bond angle of $\text{O}^2\text{C}^4\text{H}$, and bond length of C^4H were fixed at those of the free MA molecule, and C^1 , C^2 , C^3 , O^1 , O^2 , and C^4 atoms were fixed in a plane as in free MA. The two isomers found for Na(MA) have different positions of the Na atom that coordinates to the MA molecule. The binding energies ΔE with respect to separated Na and MA⁴⁰ are estimated to be 10.6 and 1.2 kcal/mol for **a** and **b**, respectively. In isomer **a**, the lengths of $\text{C}^1=\text{C}^2$ and $\text{C}^3=\text{O}^1$ are $\sim 5\%$ longer than those of the free MA molecule. In contrast, the C^2-C^3 bond length is $\sim 5\%$ shorter. These changes in bond lengths can be easily explained by considering the electron distribution in the singly occupied molecular orbital (SOMO) of Na(MA), as shown in Figure 6d. In the SOMO of isomer **a**, the electron population in the antibonding orbital over the $\text{C}^1=\text{C}^2$ and $\text{C}^3=\text{O}^1$ bonds, which is the lowest unoccupied molecular orbital (LUMO) of MA, is large because the valence 3s electron of the Na atom is transferred to the LUMO of MA. Therefore, the antibonding nature of the $\text{C}^1=\text{C}^2$ and $\text{C}^3=\text{O}^1$ bonds and the bonding nature of the C^2-C^3 bond caused by electron transfer from the Na atom are related to these bond length changes. This result can also be explained by the overlap between the Na 3s orbital and the LUMO of MA. In contrast, there are no changes of bond length in isomer **b**. This result suggests that electron transfer from the Na atom to the MA molecule does not take place in **b**. In isomer **a**, electron transfer from the Na atom enlarges the electron density at C^2 . In general, the electron density of the C^2 atom is important in the propagation of the oligomerization reaction, because the reaction proceeds by the nucleophilic attack by this atom at the C^1 atom of another MA molecule. Therefore, isomer **a** is expected to be important in anionic oligomerization.

(40) The binding energies ΔE_n of these isomers can be evaluated by $-\Delta E_n = E[\text{Na}(\text{MA})_n] - E[\text{Na}] - nE[\text{MA}]$, where $E[\text{Na}(\text{MA})_n]$ is the total energy of $\text{Na}(\text{MA})_n$; $E[\text{Na}]$ and $E[\text{MA}]$ are the total energies of Na atom and MA molecule, respectively.

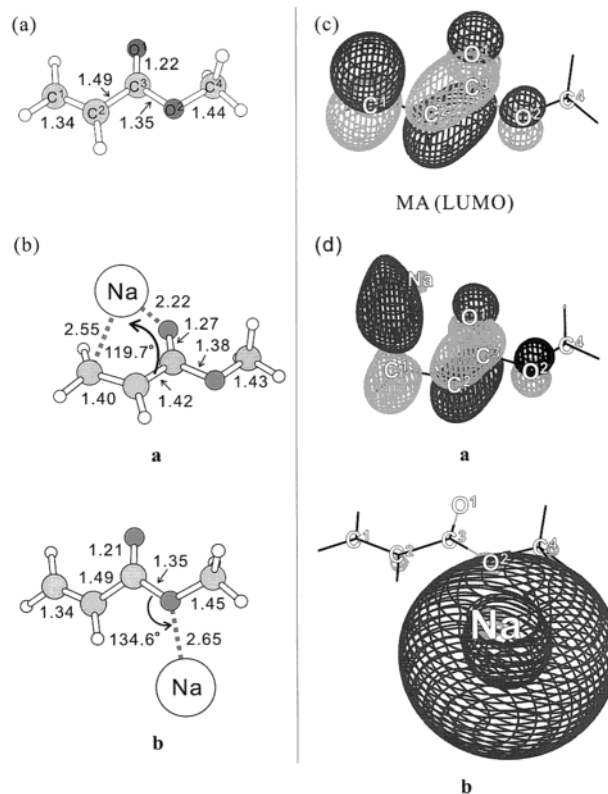


Figure 6. Optimized structures of neutral (a) *s*-cis MA and (b) Na-(*s*-cis MA) calculated at the B3LYP/6-31+G* level. Bond lengths and angles are shown in angstroms and degrees, respectively. For free MA, full geometrical optimization was performed. In the optimization for Na(MA), some of the geometrical parameters were fixed to those of the optimized free MA (see text). Contour surfaces of the square of atomic orbital coefficients of (c) LUMO for *s*-cis MA and (d) SOMOs for isomer **a** and **b** are also shown.

The vertical electron affinity of an MA molecule is expected to be slightly negative or, at least, to be no more positive than $+0.2$ eV based on the electron transmission spectroscopy.⁴¹ In the mass spectrum of $(\text{MA})_n^-$, the $(\text{MA})_3^-$ ion is produced more efficiently than $(\text{MA})^-$.⁶ Thus, it is expected that $(\text{MA})_3$ can accept the excess electron more efficiently than the MA molecule. Present calculations reveal that, despite the poor ability of MA to accept the excess electron, the valence electron of the Na atom is almost fully transferred to MA in Na(MA). Therefore, it is expected that in $\text{Na}(\text{MA})_3$ electron transfer from Na atom to $(\text{MA})_3$ takes place and induces the intracuster oligomerization reaction.

G. Comparison with the Cluster Negative Ions $(\text{MA})_n^-$ As noted in the Introduction, it is well known that the electron transfer from alkali metals initiates the anionic polymerization reaction of vinyl compounds in the condensed phase. Also, in the present cluster, the alkali metal atom is expected to act as an electron donor to the cluster of vinyl compounds. Kondow and co-workers also investigated the mass spectroscopy of various vinyl cluster anions as another model system of the oligomerization reaction.⁵⁻¹² In some systems, these two studies have given similar results. For example, the mass spectrum of acrylonitrile cluster anions⁵ has features similar to that of photoionized alkali atom-acrylonitrile clusters,¹³ and thus, the electron transfer from the metal to the clusters is concluded in the latter system.

(41) Schafer, O.; Allan, M.; Haselbach, E.; Davidson, R. S. *Photochem. Photobiol.* **1989**, *50*, 717.

By contrast, the mass spectra of $(MA)_n^-$ has little resemblance to those of photoionized $M(MA)_n$ ($M = Na, K$).⁶ In their mass spectrum, the $(MA)_5^-$ ion was most strongly observed, with no magic number at $n = 3$. It is informative to discuss the reason for this difference. The most significant difference between the MA cluster anion and the metal-MA clusters is that a counterion remains near the MA cluster anion in the latter system. It is expected that clusters containing alkali metal atoms and acrylic esters form ion pairs in present system. From the results of calculations for Na-MA, isomer **a** in Figure 6 is obtained for such an ion-pair structure. In this isomer, the Na atom coordinates near the O¹ atom and as a result the nucleophilicity of the O¹ atom is suppressed with respect to that of the C² atom. As noted above, the nucleophilicity of the C² is important in the oligomerization reaction. Therefore, the position of the Na atom in isomer **a** is favorable to anionic oligomerization. As a result, structures **1** (the precursor of the Dieckmann cyclization) and **3** (the cyclic trimer) in Scheme 1 are efficiently produced at $n = 3$. By contrast, for the MA cluster anions, the O¹ atom has sufficient nucleophilicity to possibly promote a reaction mechanism other than that seen in the present case.

5. Concluding Remarks

There have been some questions concerned with the gas-phase oligomerization reactions of vinyl compounds. In the case of acrylonitrile, studies of electron attachment to the clusters by Kondow and co-workers^{5,9-11} as well as studies of the neutral clusters with an alkali atom by the author's group¹³ revealed that formation of cyclic oligomers with a trimeric unit (process 1) is decisively important. On the other hand, for methyl acrylate, the study of ion-molecule reactions by McDonald and Chowdhury³ showed that the Dieckmann cyclization reaction (process 2) peculiar to esters is an important termination process providing a trimeric unit. Furthermore, electron-attachment studies⁶ gave no evidence of trimeric units for MA, in contrast with the other findings mentioned above.

In the present study, clusters of an alkali metal atom and acrylic ester molecules, $M(CH_2=CHCO_2R)$ ($M = Na$ and K ; $R = CH_3, C_2H_5$), have been found to undergo both process 1 and process 2 as competitive processes. These intracluster

reactions are induced by electron transfer from the alkali metal atom to acrylic esters to yield cyclic oligomers with trimeric units. In process 1, a cyclohexane derivative is produced. In process 2, Dieckmann cyclization occurs to produce a dissociated species of an ROH molecule. It has been demonstrated that process 1 is a characteristic reaction of the gas-phase cluster systems containing vinyl radical anions. Process 2 is concluded to be an additional process of dissociative cyclization, which becomes possible in the cases of acrylic esters in contrast to the case of acrylonitrile.

The marked difference between clusters composed of an alkali atom and vinyl molecules and cluster anions of vinyl molecules provides an insight into the initial step of the anionic polymerization reaction system in bulk solution. In the present metal-acrylic ester clusters, the anionic oligomerization has clearly been observed for acrylic ester molecules as in the case of acrylonitrile clusters, whereas no clear evidence was obtained in the study of free cluster anions.⁶ On the basis of theoretical calculations of the Na(MA) cluster, this difference can be ascribed to the site-specific effect in the presence of the alkali metal cation for the metal-acrylic ester clusters. The presence and the location of the counterion have been demonstrated to be crucially important in the present study. Therefore, clusters of vinyl molecules with an alkali metal atom are expected to be more promising for the study of the initial process of the anionic oligomerization reactions than other gas-phase approaches dealing with anions without counterions.

Acknowledgment. The authors acknowledge Professor Tasuku Ito for supplying us with a vacuum drybox for the preparation of the alkali metal sample rod. We also thank Dr. Toru Egawa for providing us with information on the structure of methyl acrylate. This work was partly supported by a Grant-in-Aid for Scientific Research from the Japanese Ministry of Education, Science, Sports and Culture. K. Ohshimo is supported by a Research Fellowship of the Japan Society for the Promotion of Science for Young Scientists. F.M. also acknowledges financial support from the Kurata Foundation and Mitsubishi Foundation.

JA002155C